

## Synthesis, characterization and molecular properties of *n*'-(5-m nitrophenylazosalicyliden)nicotinohydrazide

Santhi N and Sankaran KR\*.

Department of Chemistry, Annamalai University, Annamalainagar, Tamilnadu, India.

\*Corresponding Author: E-Mail: professorskrs60@gmail.com

Received: 21 Mar 2015, Revised and Accepted: 28 Mar 2015

### ABSTRACT

*N*'-(5-m-Nitrophenylazosalicyliden)nicotinohydrazide **3** is synthesized from the condensation of *N*'-5-m-nitrophenylazosalicylaldehyde **1** with nicotinohydrazide **2**. 5-m-nitrophenylazosalicylaldehyde was prepared by diazotization of *m*-nitroaniline and then the coupling reaction with salicylaldehyde. This compound was characterized by IR, <sup>1</sup>H and <sup>13</sup>C NMR spectral studies. The structure of the compound are optimized and studied by B3LYP density functional method calculations at 6-31G(d,p) basis set using Gaussian-03 software. The HOMO-LUMO energies and their energy gap and geometrical parameter were also computed

**Keywords:** Nicotinohydrazide, DFT, HOMO-LUMO, MEP.

### 1. INTRODUCTION

Hydrazide derivatives have been of great interest because of their role in natural and synthetic organic chemistry [1]. Some widely used antibacterial drugs such as furacilin, furazolidone anftivazide are known to containing hydrazone group. Hydrazone are aversalile class insecticides, anticoagulants, antitumargents, antioxidant and plant growth regulators [2-4]. Hydrazone functional group increases the lipophilicity of parent amides and results in the enhancement of absorption through biomembranes and enables them to cross bacterial and fungal membranes [5, 6]. Their metal compounds have found applications in various chemical processes like non-liner optics, sensors, medicine etc [7]. The chemistry of Schiff bases has been investigated in recent years. Schiff bases hydrazones are widely used in analytical chemistry as selective metal extracting agents as well as in spectroscopic determination of certain trasionic metals [8,9]. Schiff bases complexes have been widely studied because they have industrial, fungicide, antibacterial, anticancer and herbicidal applications [10, 11].

### 2. EXPERIMENTAL

Nicotinohydrazides was purchased from sigma Aldrich. All other chemicals were used as analytic grade. Reaction was monitored by TLC. The melting points were measured on open capillaries and are in corrected.

### 2.1. Synthesis of *N*'-(5-m-Nitrophenylazosalicyliden)nicotinohydrazide **3**

*N*'-(5-m Nitrophenylazosalicyliden)nicotinohydrazide **3** was prepared according to the literature [12]. To solution of *N*'-5-m-nitrophenylazosalicylaldehyde **1** (0.01 mol, 1.371 g) and nicotinohydrazide **2** (0.01 mol, 2.3 g) in methanol five drops of glacial acetic acid were added and the reaction mixture was refluxed for 6 h and then the mixture was poured into ice cold water. The mixture was kept overnight at room temperature. It was filtered, washed and recrystallized from methanol. Yield was found to be 84%, colour: orange; m.p. 163–165°C.

### 2.2. Spectral measurements

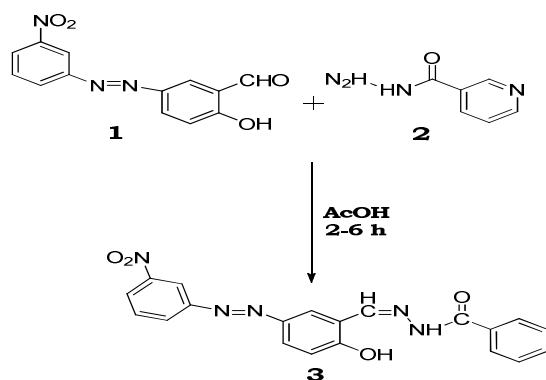
The FT-IR spectrum is recorded in the range 4000–400 cm<sup>-1</sup> with a resolution of ±4 cm<sup>-1</sup> and an accuracy of ±0.01 cm<sup>-1</sup> on Nicolet Avatar 360 FT-IR spectrometer. The sample was mixed with KBr and the pellet technique was adopted. The proton spectrum at 400 MHz and proton decoupled <sup>13</sup>C NMR spectrum at 100 MHz in DMSO-d<sub>6</sub> were recorded at room temperature on Bruker 400 MHz spectrometer using 10 mm sample tube, samples were prepared by dissolving about 10 mg of the sample in 0.5 mL of DMSO-d<sub>6</sub> containing a few drops at TMS for <sup>13</sup>C.

### 2.3. Computational studies

Geometry optimization was carried out according to density functional theory available in Gaussian-03 package using B3LYP/6-31G(d,p) basis set [13].

### 3. RESULTS AND DISCUSSION

The N'-(5-m-Nitrophenylazosalicyliden) nicotino-hydrazone **3** is obtained by refluxing 5-m-nitrophenylazosalicylaldehyde **1** with nicotino-hydrazone **2** and 5 drops of acetic acid in methanol (Scheme 1). All the synthesized compounds are characterized by the FT-IR and the high-resolution  $^1\text{H}$  and  $^{13}\text{C}$  NMR spectra and analyzed. The theoretical vibrational frequencies of the hydrazone **3** is calculated using DFT method with 6-31G(d,p) basis set and scaled by a factor 0.9614.



**Scheme - 1: Synthetic route of N'-(5-m-Nitrophenylazosalicyliden)nicotino-hydrazone 3.**

**Table - 1: IR experimental and theoretical values of compound 3**

IR Frequency	
Experimental	Theoretical
3357	3404
3196	3225
3030	3030
2918	2948
1618	1600
1528	1499
1488	1470

The prominent peaks in the range 3430–3190, 1650–1800 and 1640–1560  $^{14}$   $\text{cm}^{-1}$  in the IR spectrum are attributed to  $\nu_{\text{N-H}}$  and  $\nu_{\text{O-H}}$ ,  $\nu_{\text{C=O}}$  and  $\nu_{\text{C=N}}$  and  $\nu_{\text{C=C}}$  modes respectively. The observation of lower  $\nu_{\text{C=O}}$  is due to the extended conjugation of C=O group with the nearby pyridine ring. The bending vibration of the O–H group appeared around 1350  $\text{cm}^{-1}$  in all the hydrazides. The sharp peak around 3020  $\text{cm}^{-1}$  in

the IR spectrum of **3** due to the aromatic  $\nu_{\text{C-H}}$  mode. In hydrazone strong peak for N=N group is observed at 1480  $\text{cm}^{-1}$  [15]. Aromatic C–H out-of-plane bending vibration appeared around 840 and 700  $\text{cm}^{-1}$  [16]. The experimental and calculated (DFT) IR spectral data of **3** is displayed in Table 1 and the IR spectrum of hydrazone **3** is shown in Figure 1.

#### 3.1. Spectral ( $^1\text{H}$ and $^{13}\text{C}$ NMR) Calculation

The signals in the  $^1\text{H}$  NMR spectrum (Figure 2) were assigned based on their positions, integrals, multiplicities and on comparison with those signals of 5-phenylazosalicylaldehyde. In  $^{13}\text{C}$  NMR spectrum (Figure 3) quaternary carbons can be easily distinguished from other carbons based on small intensities. The  $^1\text{H}$  and  $^{13}\text{C}$  NMR chemical shifts were determined theoretically by DFT method in DMSO- $d_6$  using the basis set B3LYP/6-311+G(2d,p) GIAO and the salvation model PCM (SCRF=PCM) [17]. The  $^1\text{H}$  and  $^{13}\text{C}$  chemical shifts relative to reference material TMS are determined from the shielding tensors using the scale factors 31.8821 and 182.4656 respectively and they are listed in Table 1 itself. The scale factors are based on the reference compounds used as well as on the basis set employed for DFT calculation. Theoretically determined  $^1\text{H}$  chemical shifts are generally high when compared to experimental values and large derivatives are noted on some protons. The experimental  $^{13}\text{C}$  chemical shifts are however closer to the theoretical values. Experimental and computational  $^1\text{H}$  and  $^{13}\text{C}$  NMR spectral data of hydrazone **3** are listed in table 2 and 3.

**Table - 2:  $^1\text{H}$  NMR experimental and theoretical values of compound 3**

$^1\text{H}$ NMR Values (ppm)		
protons	Observed	Theoretical
H-2	9.11	9.30
H-4	8.31	8.86
H-5	7.61	7.93
H-6	8.79	9.15
H-11	8.79	8.65
H-14	7.17	7.53
H-15	8.00	8.57
H-17	8.37	8.62
H-22	8.55	9.34
H-23	-	-
H-24	8.37	8.94
H-25	7.89	7.95
H-26	8.37	8.91
CH <sub>3</sub>	-	-

**Table - 3: <sup>13</sup>C NMR experimental and theoretical values of compound 3**

Experimental and theoretical values of <sup>13</sup> C NMR Spectra		
Carbons	Obs.	DFT
C-2	148.59	153.48
C-3	129.71	134.82
C-4	135.54	144.12
C-5	123.72	129.54
C-6	152.28	160.57
C-7	161.70	167.73
C-11	146.44	153.56
C-12	119.86	123.82
C-13	161.11	172.45
C-14	117.48	122.37
C-15	126.61	145.02
C-16	144.77	152.77
C-17	123.72	122.51
C-21	152.49	160.11
C-22	115.06	134.98
C-23	148.56	156.80
C-24	124.73	132.08
C-25	131.02	135.68

### 3.2. Geometric parameters

From the optimized structures, geometrical parameters were derived (Table 4). The calculated bond lengths of C3–C7 and C11–C12 are in agreement with the bond lengths expected for a single bond. The observed torsional angles indicate all the atoms lie in the same plane except the pyridine ring. The torsional angles C4–C3–C7–N9 [ $\approx 158^\circ$ ] and C2–C3–C7–N9 [ $\approx 24^\circ$ ] indicate the distortion of pyridine ring from other moieties. Further, the torsional angles C2–C3–C7–O8 [ $\approx 156^\circ$ ] and C4–C3–C7–O8 [ $\approx 21^\circ$ ] also support the distorted nature of pyridine ring from other moieties lying in the same plane.

**Table - 4: Geometrical parameters (Bond length, Bond angle, bond Torsional angle) of compound 3**

Geometric parameters	
Bond length	
C3–C7	1.50
C7–O8	1.22
C7–N9	1.39
N9–N10	1.36
N10–C11	1.29

C11–C12	1.45
C13–O18	1.34
C16–N19	1.41
N19–N20	1.26
N20–C21	1.42
O18–H18	0.99
C24–F27/C24–C27	-
C23–C27/C23–N27	1.47
Bond angle	
C3–C7–O8	122.7
C3–C7–N9	114.9
O8–C7–N9	122.4
C7–N9–N10	119.2
N9–N10–C11	119.6
N10–C11–C12	120.6
H18–O18–C13	109.5
C16–N19–N20	115.3
N19–N20–C21	114.3
Torsional angle	
C4–C3–C7–N9	-158.1
C4–C3–C7–O8	21.3
C2–C3–C7–O8	-156.5
C2–C3–C7–N9	24.0
C3–C7–N9–N10	179.5
O8–C7–N9–N10	1.0
C7–N9–N10–C11	-174.7
N9–N10–C11–C12	-179.8
N10–C11–C12–C13	-0.5
N10–C11–C12–C17	179.7
C11–C12–C13–O18	-0.0
C12–C13–O18–H18	-0.1
C17–C16–N19–N20	0.2
C15–C16–N19–N20	-179.8
C16–N19–N20–C21	180.0
N19–N20–C21–C22	-179.8
N19–N20–C21–C26	0.2

### 3.3. HOMO-LUMO energies dipole moment

HOMO-LUMO energies and dipole moments for the hydrazide 3 was calculated by using B3LYP/6-31G(d,p) basis set in Gaussian-03 package. HOMO-LUMO pictures are reproduced in figure 1 and 2 and From it is seen that the introduction of electron withdrawing nitro substituents at the para and meta position of phenyl ring decreases the energies of both HOMO and LUMO orbitals whereas electron releasing

methyl substituents increase the energies of both HOMO and LUMO orbitals. Introduction of substituents at the phenyl ring decreases the energy gap ( $\Delta E$ ).

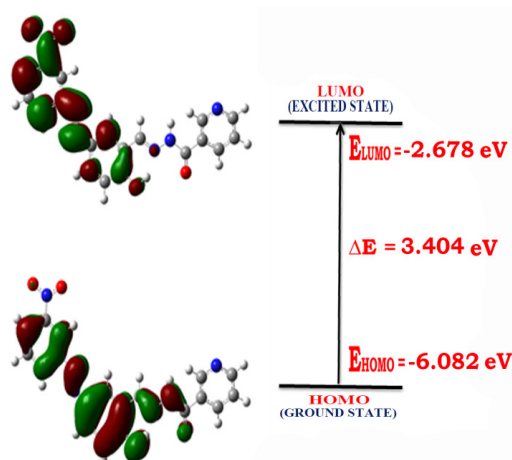


**Figure - 1: HOMO-LUMO picture of compound 3**

The dipole moment is higher in hydrazide **3** whereas in other compounds the dipole moments are lower compared to the parent hydrazide **1**. The electronic chemical potential ' $\mu$ ' which is a characteristic of electronegativity defined by Parr and Pearson [18] and hardness ' $\eta$ ' have been calculated using the formulae  $\mu = -\frac{1}{2} [E_{\text{HOMO}} + E_{\text{LUMO}}]$ ,  $\eta = \frac{1}{2} [E_{\text{LUMO}} - E_{\text{HOMO}}]$  and the values are also listed in table 1. The higher HOMO energy corresponds to the more reactive molecule in the reactions with electrophiles, while lower LUMO energy is essential for molecular reactions with nucleophiles [19]. The hardness corresponds to the gap between the HOMO and LUMO orbitals. The larger the HOMO-LUMO energy gap, the harder the molecule [20]. Hardness measures the resistance to change in the electron distribution in a molecule. If lower is the HOMO-LUMO gap, there is easy flow of electrons to the higher energy state making it softer and more reactive [HSAB principle].

HOMO orbitals are mainly derived from p<sub>z</sub> orbitals of carbon, nitrogen and oxygen atoms except p<sub>z</sub> orbitals of pyridine ring in all the hydrazides. In hydrazide **3** in addition to the pyridine ring the p<sub>z</sub> orbitals of substituent atoms are also not participated in the construction of HOMO orbitals. The LUMO orbitals are mainly derived from p<sub>z</sub> orbitals of carbon. In nitro derivative **3** the p<sub>z</sub> orbitals of pyridine ring, nitrogen atoms N9 and N10, carbonyl group, C(14), C(11) and C(26) carbon atoms are not participated in the formation of LUMO orbital.

### 3.4. MEP surfaces

Three dimensional distribution of MEP (molecular electrostatic potential) is highly useful in predicting the reactive behaviour of the molecule. The molecular electrostatic potential MEP surface is an overlaying of the electrostatic potential on to the isoelectron density surface. This is a valuable tool for describing over all molecule charge distribution as well as anticipating sites of electrophilic addition. The molecular electrostatic potential surface (MEP) has been plotted for hydrazides **3** and the diagram is given in figure 2. Region of negative charge (red colour) is seen around the electronegative oxygens O(8) and O(18) in all the hydrazides. In hydrazide **3** in addition red colour is seen at oxygen atoms of nitro group also. The red colour region is susceptible for electrophilic attack. Blue colour (around nitrogen atoms) represents strongly positive region and the predominant green region in the MEP surfaces corresponds to a potential half way between the two extremes red and blue region in hydrazide.

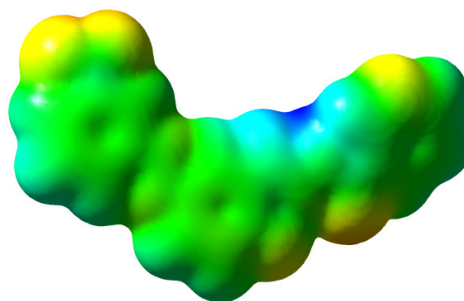


**Figure - 2: MEP diagrams of compound 3.**

## 4. CONCLUSIONS

The hydrazide **3** is synthesized and characterized by spectral studies. Theoretical FT-IR spectral frequencies are in good agreement with experimental data. The molecular structure of the hydrazide **3** is optimized and the calculated geometrical parameter are tabulated. The proton and carbon chemical shifts are calculated using the GIAO method in DFT calculation. The calculated chemical shifts are in good agreement with the experimental once. The HOMO-LUMO picture of the hydrazide and the MEP layout is also presented.

## 5. REFERENCES

1. Williams DA and Lemke TL. **Foyes principles of medicinal chemistry, 5 th edn. Lippincott Williams and wilkins, philadelphia, 2002.**
2. Shabani F and Gnamnamy S. **J.Chem.Pharma.Res., 2010; 2: 1-6.**

3. Chohan ZH, Arif M, Shafiq Z, Yaqub M, Supuran CT. **J.Enzym.Inhib.Med.chem.**, 2006; 21: 95-103.
4. Manimekalaia A, Saradhadevia N and Thiruvalluvar A. **Spectrochimica Acta Part A: Molecular and Biomolecular Spectroscopy.**, 2010; 77: 687-695.
5. Madhukar A, Kannappan N, Deep A. Kumar P, Kumar M and Prabhaka V. **Int. J. Chem. Tech. Research.**, 2009; 1: 1376.
6. Jha KK, Samad A, Kumar Y, Shaharyar M, khosa RL, Jain J, Kumar V and Sing P. **Eur. J. Med. Chem.**, 2010; 45: 4963.
7. Bakir M, Hassan I, Johnson T, Brown O, Green O, Gyles C and Coley MD. **J. Mol. Struct.**, 2004; 688: 213-222.
8. Gallego M and Garlia VM. **Analyst.**, 1979; 104: 613-619.
9. Gallego M, Garlia VM, Valcancel M, Pino F, **Microchem.J.**, 1978; 23: 353-359.
10. Jayabalakrishan C and Natarajan K. **Synth. React. Inorg. Met-Org Chem.**, 2001; 31: 983-995.
11. Maiti A and Ghosh S. **Indian J.Chem.**, 1989; 29: 980-983.
12. Odabasoglu M, Albayrak C, Ozkanca R, Aykan FZ and Lonecke P. **J. Mol. Struct.**, 2007; 840: 71-89.
13. Frisch MJ, Trucks GW, Schlegel HB, Scuseria GE, Robb MA, Cheeseman V.G. Zakrzewski, J.A. Montgomery Jr., R.E. Stratmann, J.C. Burant, S. Dapprich, J.M. Millam, A.D. Daniels, K.N. Kudin, M.C. Strain, O. Farkas, J. Tomasa, V. Barone, M. Cossi, R. Cammi, B. Mennucci, C. Pomeli, C. Adamo, S. Clifford, J. Ochterski, G.A. Peterson, P.Y. Ayala, Q. Cui, K. Morokuma, P. Salvador, J.J. Dannenberg, D.K. Malick, A.D. Rabuck, K. Raghavachari, J.B. Poresman, J. Cioslowski, J.N. Ortiz, A.G. Babboul, B.B. Stefavov, G. Liu, A. Liashenko, P. Piskorz, I. Komaromi, R. Gomperts, R.L. Martin, D.J. Fox, T. Keith, M.A. Allaham, C.Y. Peng, A. Nanayakkara, M.W. Wong, J.L. Anders, C. Gonzales, M. Challacombe, P.M. Gill, B. Johnson, W. Chen, M. Head-Gordon, E.S. Replogle, J.A. **Peple, Gaussian 98, Revision A. 9, Pittsburg, Pa: Gaussian IC, 2001.**
14. Silverstein RM and Webster FX. **Spectrometric identification of organic compounds**, 6<sup>th</sup> Ed., John Wiley and Sons, New York, 1996.
15. Kemp W. **Organic spectroscopy, The Macmillan Press Ltd.**, 1975; 14: 1375-1377.
16. Dyer JR. **Applications of absorption spectroscopy of organic compounds**, Prentice-Hall of India (P) Limited, New Delhi, 1969; 75.
17. Miertus S and Tomasi, J. **Chem. Phys.** 1982; 65: 239-245.
18. Parr RG and Pearson RG. **J. Am. Chem. Soc.** 1983; 105: 7512.
19. Rauk A. **Orbital interaction theory of organic chemistry**, 2<sup>nd</sup> edn., John Wiley and sons, Newyork, 2001; 34.
20. Pearson RG. **J. Am. Chem. Soc.**, 1985; 107: 6801.